SMA-SH: Modified styrene maleic acid copolymer for functionalization of lipid nanodiscs

Lindhoud, S.; Dias Ribeiro De Carvalho, V.I.; Pronk, JW; Aubin, ME

DOI
10.1021/acs.biomac.6b00140

Publication date
2016

Document Version
Final published version

Published in
Biomacromolecules

Article

pubs.acs.org/Biomac

SMA-SH: Modified Styrene–Maleic Acid Copolymer for Functionalization of Lipid Nanodiscs

Simon Lindhoud,* Vanessa Carvalho, Joachim W. Pronk, and Marie-Eve Aubin-Tam*

Department of Bionanoscience, Kavli Institute of Nanoscience, Delft University of Technology. Lorentzweg 1, Delft 2628 CJ, The Netherlands

Supporting Information

ABSTRACT: Challenges in purification and subsequent functionalization of membrane proteins often complicate their biochemical and biophysical characterization. Purification of membrane proteins generally involves replacing the lipids surrounding the protein with detergent molecules, which can affect protein structure and function. Recently, it was shown that styrene–maleic acid copolymers (SMA) can dissolve integral membrane proteins from biological membranes into nanosized discs. Within these nanoparticles, proteins are embedded in a patch of their native lipid bilayer that is stabilized in solution by the amphipathic polymer that wraps the disc like a bracelet. This approach for detergent-free purification of membrane proteins has the potential to greatly simplify purification but does not facilitate conjugation of functional compounds to the membrane proteins. Often, such functionalization involves laborious preparation of protein variants and optimization of labeling procedures to ensure only minimal perturbation of the protein. Here, we present a strategy that circumvents several of these complications through modifying SMA by grafting the polymer with cysteamine. The reaction results in SMA that has solvent-exposed sulfhydrils (SMA-SH) and allows tuning of the coverage with SH groups. Size exclusion chromatography, dynamic light scattering, and transmission electron microscopy demonstrate that SMA-SH dissolves lipid bilayer membranes into lipid nanodiscs, just like SMA. In addition, we demonstrate that, just like SMA, SMA-SH solubilizes proteoliposomes into protein-loaded nanodiscs. We covalently modify SMA-SH-lipid nanodiscs using thiol-reactive derivatives of Alexa Fluor 488 and biotin. Thus, SMA-SH promises to simultaneously tackle challenges in purification and functionalization of membrane proteins.

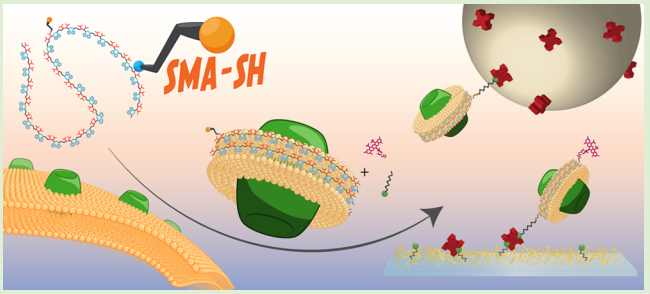

Biochemical and biophysical approaches to study membrane proteins must often overcome challenges in protein purification and functionalization. Purification of membrane proteins generally involves cell lysis, isolation of the membranes, followed by detergent-induced solubilization of the proteins in the membrane. During this step, the lipids surrounding the transmembrane domains are largely replaced by a detergent micelle, which enables purification of the proteins using standard procedures.[1] However, membrane proteins may attract specific lipids to modulate their structure and function,[2−5] which highlights the importance of their native environment within the membrane. Consequently, detergent-induced stripping of lipids from membrane proteins can be detrimental to their structure and function and may abolish their reconstitution or interactions with other proteins.

Reconstitution of detergent-solubilized proteins into native-like, albeit artificial, lipid bilayers of liposomes[6] or membrane scaffold protein-based nanodiscs facilitates their biophysical characterization.[7,8] In addition, in order to characterize interactions with other proteins, substrates, and ligands, those methods frequently require the reconstituted proteins to be immobilized onto a surface, such as a glass coverslip for total internal reflection fluorescence microscopy,[9] a sensor chip for surface plasmon resonance,[10,11] or mica for atomic force microscopy.[12] Although functionalized lipids may be incorporated in artificial lipid bilayers during reconsitution,[6,9] specific immobilization is generally mediated by covalently attached functional compounds, such as biotin. Similarly (single-molecule), detection of proteins by fluorescence microscopy often involves covalent attachment of dye labels.[13−16] Such conjugations with functional compounds require careful optimization of the reactions and demonstration that they do not compromise protein structure and function. These steps are laborious in the case of soluble proteins and even more demanding in the case of membrane proteins.

Recently, copolymers of styrene and maleic acid (SMA) were highlighted as agents that can be used for detergent-free solubilization of membrane proteins.[17−23] This amphipathic polymer dissolves membranes into disc-shaped particles that contain a patch of lipid bilayer membrane that is surrounded by a bracelet of polymer molecules.[10,17] During SMA-induced solubilization of biological membranes, integral membrane proteins may become embedded in the discs within their native

Received: January 28, 2016
Revised: March 11, 2016
Published: March 14, 2016

DOI: 10.1021/acs.biomac.6b00140
Biomacromolecules 2016, 17, 1516−1522

lipid bilayer. Subsequently, conventional purification approaches, such as affinity chromatography and gel filtration strategies, may be used to purify nanodiscs that are loaded with the protein of interest from excess polymer, empty discs and nanodiscs that are loaded with other proteins. This direct extraction of membrane proteins within their native lipid environment facilitates the analysis of lipids that surround the protein.[23,24] Thus, SMA is a versatile tool in membrane protein research.[10] However, as such, SMA does not facilitate the conjugation of functional groups to the membrane proteins, which is often required for their biochemical and biophysical characterization.

Here we propose a strategy for preparation of modified SMA that can be used for purification and conjugation of membrane proteins and obviates the need for their genetic engineering and labeling. The anhydride form of SMA (styrene-maleic anhydride; SMAnh) is the starting point for this modification, which exploits the reactivity of maleic anhydride toward alcohols and amines. This reactivity has been used to prepare biologically active conjugates of SMA with small molecules, like fluorophores, drugs, and proteins.[25−27] However, to our knowledge, at present, this reaction has not been used to modify SMA for use in membrane protein solubilization. Many compounds that are commonly used for conjugating to proteins, such as fluorophores and biotin, are available as amine-derivatives. Although these could be used to directly modify SMAnh, those compounds are generally expensive. The price tag on using functionalized SMA for preparative purposes is considerable, especially because solubilization of biological membranes requires excess of SMA. Furthermore, each distinct application potentially requires a different functional group and, thus, asks for specific preparations of functionalized SMA.

We designed and established a low-cost method for preparation of a SMA variant that can be used to solubilize membrane proteins and serve as a versatile intermediate for functionalization. This SMA variant is prepared by partially grafting the polymer with cysteamine (2-aminoethanethiol; NH_2C_2SH). Hydrolysis of the remaining maleic anhydride moieties results in SMA that has solvent-exposed sulfhydrils: SMA-SH. Following purification of the protein of interest in an SMA-SH nanodisc, the sulfhydril groups of the polymer bracelet can be further functionalized with a thiol-reactive derivative of a functional group of interest.

We show that SMA-SH is easy to prepare and that this modified polymer dissolves lipid bilayer membranes into nanosized discs that can be functionalized with thiol-reactive probes.

MATERIALS AND METHODS

Preparation of SMAnh-SH and SMA-SH. Styrene-maleic anhydride copolymer with a styrene to maleic anhydride ratio of 2:1 and MW 7500 g/mol (SMAnh) was purchased from Polysciences. A 100 mg/mL solution of SMAnh was prepared in a 50 mL PPCO centrifuge tube (Nalgene) by dissolving 1 g of SMAnh in 10 mL of anhydrous DMF (Sigma). The solution was bubbled with nitrogen to drive out oxygen and to ensure mixing during the reaction, which was carried out at ambient temperature. To this solution, 15.1, 30.2, or 45.3 mg of cysteamine-HCl (Sigma) was added from a freshly prepared cysteamine stock solution in DMF to produce SMAnh-SH_1, SMAnh-SH_2 or SMAnh-SH_3, respectively. A total of 700 μL of triethylamine (Et_3N; Sigma) was added to the reaction, followed by incubation during 30 min, after which the polymer was precipitated by the addition of 25 mL of 600 μM acetic acid (Sigma). The polymer was harvested by centrifugation at 35000 × G, followed by several cycles of washing the pellet in 600 μM acetic acid and centrifugation, to remove traces of DMF. Finally, the polymer was lyophilized and stored at room temperature until use.

To hydrolyze SMAnh and SMAnh-SH_x, 10 mg/mL suspensions of SMAnh-SH_x were prepared in 0.1 M borate buffer, pH 8.5, with 100 mM DTT, in 15 mL screw-cap tubes, and a small stirring magnet was added. The suspensions were kept at 100 °C, for up to 4 h, while stirring. The resulting SMA and SMA-SH_x solutions were transferred to dialysis tubing with a molecular weight cutoff of 3.5 kDa (Spectrapor) and extensively dialyzed against 20 mM Tris·HCl pH 8 with 1 mM DTT, followed by 5 mM Tris·HCl, pH 8.0, with 1 mM DTT. Subsequently, the solutions were lyophilized. Dry polymer was dissolved to a concentration of 60 mg/mL in 20 mM Tris·HCl pH 8.0, 10 mM DTT, and stored at −20 °C until use.

Determination of Thiol Content. A HiTrap desalting column (GE-Healthcare) was used to purify 500 μL of 10 mg/mL SMA-SH_x from DTT just before determination of thiol content using dithionitrobenzoicacid (DTNB; Sigma). A 20 mM stock solution of DTNB was prepared in DMSO and stored at −20 °C. A DTNB working solution was prepared freshly by diluting the DTNB stock solution 200× in 0.2 M Tris·HCl, pH 7.5. A 250 μL aliquot of sample was diluted into 750 μL of the DTNB working solution and incubated for 30 min before measurement of absorbance at 412 nm using a Denovix DS-11+ spectrophotometer. The thiol concentration was calculated using the molar extinction coefficient of DTNB at 412 nm (14150 M^{-1} cm^{-1}). Absorption values for SMA-SH_x stock solutions obtained at 260 nm were used to correct the thiol concentration for differences in polymer concentration between samples.

Assessment of Liposome Dissolution. For preparation of liposomes, a volume of 1,2-dimyristoil-*sn*-glycero-3-phosphocholine in chloroform (Avanti Polar Lipids; DMPC) was dried under a stream of nitrogen, followed by incubation under vacuum for several hours. Subsequently, the dry lipids were suspended to a concentration of 100 mg/mL in 20 mM Tris·HCl, pH 8.0, and 200 mM NaCl by sonication in a bath sonicator (Branson), and stored at −20 °C until use. Time-dependence of SMA- and SMA-SH-induced liposome dissolution was monitored by the intensity of light scattered at a 90° angle by an illuminated solution of liposomes using a Cary Eclipse spectrofluorometer (Varian) equipped with a Peltier temperature controller. A 0.05 mg/mL solution of DMPC liposomes was prepared by dilution of the 100 mg/mL DMPC stock solution into 20 mM Tris·HCl, pH 8.0, 200 mM NaCl and 2 mM DTT, followed by sonication. A disposable 4×Optical acrylic cuvette (Sarstedt) holding 2 mL of the liposome solution was placed in the fluorometer. A stirring magnet was placed in the cuvette and stirred at maximum speed to ensure mixing, and the solution was equilibrated at the set temperature for at least 5 min before addition of SMA or SMA-SH_x to a final concentration of 0.15 mg/mL. Excitation and emission wavelengths of the fluorometer were set identically, excitation and emission slits were set to 10 nm, and scattered light was filtered through the 3%T attenuator emission filter before detection.

Purification and Size Determination of SMA- and SMA-SH_x-lipid Nanodiscs. SMA-DMPC nanodiscs and SMA-SH_x-DMPC nanodiscs were prepared by mixing 5 mg/mL DMPC in 20 mM Tris·HCl pH 8.0, 200 mM NaCl and 10 mM DTT with 15 mg/mL SMA or SMA-SH_x, followed by incubation at 37 °C for at least 10 min. Lipid nanodiscs were separated from free polymer by gel-filtration on a Superdex 200 Increase 10/30 GL column (GE Healthcare Life Sciences) that was equilibrated in 20 mM Tris·HCl, pH 8.0, 200 mM NaCl, and 2 mM DTT, at 4 °C. DTT was omitted in case of purification of lipid nanodiscs for labeling with thiol-reactive probes. The column was calibrated using the Gel Filtration Calibration Kit HMW (GE Healthcare Life Sciences).

A Zetasizer ZS instrument (Malvern) was used to determine the size of particles by dynamic light scattering (DLS). Samples were briefly degassed under vacuum and equilibrated for 300 s at 25 °C before the start of the measurement. Default settings in the software were used for optimizing measurement settings and duration. "Multiple narrow modes" analysis of the correlation data was used

DOI: 10.1021/acs.biomac.6b00140
Biomacromolecules 2016, 17, 1516−1522

to obtain intensity-based particle size distributions, assuming spherically shaped particles.

Carbon-coated 400 square mesh copper grid from Electron Microscopy Sciences were glow-discharged for 30 s. A single droplet of 3 μL of sample was applied to the grid and removed after 60 s by blotting with filter paper (Whatman). The grid was briefly washed with water, and excess water was removed by blotting with filter paper prior to staining with 3 μL of 2% uranyl acetate during 60 s. Excess of staining was removed by blotting with filter paper and the grid was dried at room temperature. TEM was performed using a Philips CM200 (200 kV). The micrographs were imaged with a TemCam-F416 4 kkD (TVIPS) and recorded at 57000× magnification using EM-MENU software. Particle sizes of 200 manually and randomly picked particles were determined using ImageJ using a pixel size of 0.186 nm.

Preparation of SMA-bR and SMA-SH_3-bR Nanodiscs. A suspension of 1 mg/mL of lyophilized purple membrane (PM) from wild-type *Halobacterium salinarum* R1 (Actilor) in phosphate buffered saline, with 2 mg/mL DMPC was prepared by sonication. Subsequently, *n*-octyl glucoside (nOG; Anatrace) was added up to 20 mg/mL from a 10% solution in H_2O, followed by incubation at ambient temperature during 3 h in the dark to solubilize bacteriorhodopsin (bR) from PM. Reconstitution of nOG-solubilized bR into DMPC liposomes was induced by addition of an equal volume of Bio-Beads SM-2 (Bio Rad) that were pretreated with methanol and equilibrated in 20 mM Tris·HCl, pH 8, 200 mM NaCl. Following incubation at ambient temperature during 16 h with gentle agitation, bR-DMPC proteoliposomes were eluted from the Bio-beads. Tris·HCl was added to a final concentration of 20 mM, and DTT was added to 5 mM. SMA-bR and SMA-SH_3-bR nanodiscs were formed by addition of 6 mg/mL of SMA or SMA-SH_3, respectively, followed by incubation at 37 °C during at least 1 h. Aggregates were removed by centrifugation for 8 min at 16000 × G. SMA-bR and SMA-SH_3-bR nanodiscs were analyzed with gel filtration by injecting samples of 500 μL on a Superdex 200 Increase column that was equilibrated in 20 mM Tris·HCl, pH 8, with 200 mM NaCl.

Labeling of SMA-SH_3-Lipid Nanodiscs with Thiol-Reactive Probes. SMA-SH_3-DMPC nanodiscs were prepared as described above. SMA-SH_3-DMPC nanodiscs containing 1% Atto647N-labeled 1,2-dimyristoil-*sn*-glycero-3-phosphoethanolamine (Atto647N-DMPE; Atto-Tec), were prepared by mixing 5 mg/mL DMPC + 1% Atto647N-DMPE with 15 mg/mL SMA-SH_3. Lipid-nanodiscs were separated from free polymer by gel-filtration on a Superdex 200 Increase 10/30 GL column (GE Healthcare Life Sciences) that was equilibrated in 20 mM Tris·HCl pH 8.0, 200 mM NaCl. Purified SMA-SH_3-lipid nanodiscs were labeled during 16 h at 4 °C with 10−20× molar excess of Alexa Fluor 488 C_5 maleimide (ThermoFischer Scientific), maleimide-PEG11-biotin (ThermoFischer Scientific) or biotin-maleimide (Sigma-Aldrich), added from 14 mM stock solutions in DMSO. Labeled SMA-SH_3-lipid nanodiscs were separated from nonreacted probes using PD10 desalting columns (GE-Healthcare Life Sciences) equilibrated in 20 mM Tris·HCl, pH 8.0, 200 mM NaCl and 2 mM DTT. Biotinylated SMA-SH_3-lipid nanodiscs were concentrated 10× using Amicon spin-filters with a molecular weight cutoff of 10 kDa (Millipore).

Fluorescence Spectroscopy. Fluorescence measurements were carried out using quartz cuvets (Hellma) in a Cary Eclipse spectrofluorometer equipped with a Peltier temperature controller. Absorption values at 495 and 644 nm were determined for preparations containing A488-labeled SMA-SH_3-DMPC nanodiscs, A488-labeled SMA-SH_3-[DMPC + 1% Atto647N-DMPE] nanodiscs, and SMA-[DMPC + 1% Atto647N-DMPE] nanodiscs. Using those values, the concentrations of A488-labeled SMA-SH_3-DMPC nanodiscs and SMA-[DMPC + 1% Atto647N-DMPE] nanodiscs were set to the concentration of A488-labeled SMA-SH_3-[DMPC + 1% Atto647N-DMPE] nanodiscs.

Interaction between biotinylated SMA-SH_3-[DMPC + 1% Atto647N-DMPE] nanodiscs and avidin was assessed using the DyLight Reporter Solution from the Fluorescence Biotin Quantitation Kit (ThermoFischer Scientific), which contains DyLight488-labeled avidin (D488-avidin). This solution was diluted 400× in 20 mM Tris·HCl, pH 8.0, 200 mM NaCl, and 2 mM DTT. The 5 μL biotinylated SMA-SH_3-[DMPC + 1% Atto647N-DMPE] nanodiscs were added to 1 mL of D488-avidin solution and to 1 mL of D488-avidin solution + 0.1 μM Biocytin (ThermoFischer Scientific). Fluorescence emission spectra were collected upon excitation at 475 nm.

RESULTS AND DISCUSSION

SMA-SH is Obtained by Grafting of SMA with Cysteamine. The initial step for preparation of SMA-SH is the formation of an amide bond between maleic anhydride groups in the polymer and the amine group of cysteamine (SMAnh-SH; Scheme 1). Here, we use SMAnh with a styrene

Scheme 1. Reaction Scheme for the Preparation of SMA-SH

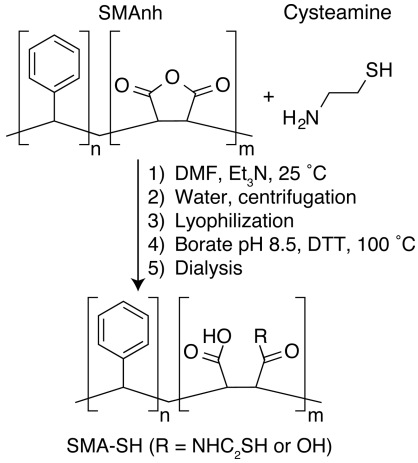

to maleic anhydride ratio of 2:1, but the same procedure can be applied to SMAnh-copolymers with different compositions. Using a value of 7500 g/mol for the molecular weight of SMAnh, we carry out this reaction with molar ratios of SMAnh to cysteamine of 1:1, 1:2, and 1:3, respectively. The products of these reactions are denoted by "-SH_x", in which *x* is 1, 2, or 3, respectively. Note that SMAnh preparations are typically polydisperse.[10] Polydisperse polymers are characterized by broad size distributions and may also contain very short chains and monomers.[28] After the reaction with cysteamine, such short chains are lost during the precipitation and dialysis steps. Consequently, the actual molar ratio of cysteamine to SMA cannot be precisely controlled. Ultimately, the heterogeneous nature of the polymer results in a seemingly low yield of SMAnh-SH_x.

Hydrolysis of maleic anhydride into maleic acid is required for use of SMA to solubilize membrane proteins. This typically involves refluxing of the polymer suspension in an alkaline solution. To prevent irreversible oxidation of thiols on the SMAnh-SH compound, this hydrolysis step must be performed below pH 9. We therefore carry out the hydrolysis of SMAnh-SH in borate buffer, pH 8.5, and in the presence of dithiothreitol (DTT). A 10 mg/mL SMAnh-SH suspension is prepared in a closed polypropylene tube and is heated at 100 °C during 4 h while stirring continuously to disperse particles.

Gel filtration was used to purify SMA-SH from borate buffer and DTT prior to determination of the thiol concentration. Figure 1 shows that the concentration of sulfhydril groups increases with the amount of cysteamine added during the reaction. Owing to the heterogeneous nature of the polymer in terms of length and "sequence", it is impossible to tune the

DOI: 10.1021/acs.biomac.6b00140
Biomacromolecules 2016, 17, 1516−1522

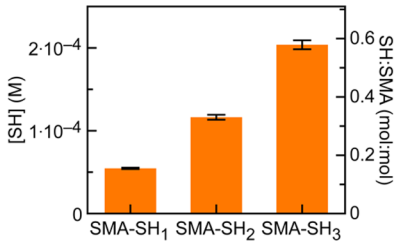

Figure 1. Ratio of SMAnh to cysteamine used in the reaction tunes the amount of sulfhydrils in SMA-SH. The concentration of sulfhydrils in SMA-SH$_x$ solutions of 2.6 mg/mL was determined using the Ellman's assay; error bars show the standard deviation of duplicate measurements. The concentration of polymer was calculated using a molecular weight of 7500 g/mol.

reaction to yield singly grafted polymer molecules. Instead, the product of the reaction is a mixture of polymer molecules that are grafted to different extents; some polymer molecules may carry several sulfhydrils, whereas others have none. We show below that, despite this heterogeneity, SMA-SH$_1$, SMA-SH$_2$, and SMA-SH$_3$ are all capable of dissolving lipid bilayer membranes into nanosized discs, just like SMA.

SMA-SH Dissolves Lipid Bilayer Membranes into Nanosized Discs. To test the effect of modification of SMA with cysteamine, we first assess the membrane dissolving properties of SMA-SH$_x$. A decrease in the turbidity of a solution of liposomes upon addition of excess polymer over lipids (3:1 w/w) hallmarks SMA-induced dissolution of lipid bilayer membranes and induces formation of discs with diameters of about 10 nm.[10,29] We use a fluorometer to monitor the corresponding kinetics of this process from the change in the intensity of 400 nm light scattered at a 90° angle by a solution of 1,2-dimyristoil-*sn*-glycero-3 phosphocholine (DMPC; T_m = 24 °C) liposomes at 20 °C. Figure 2 shows that the intensity of

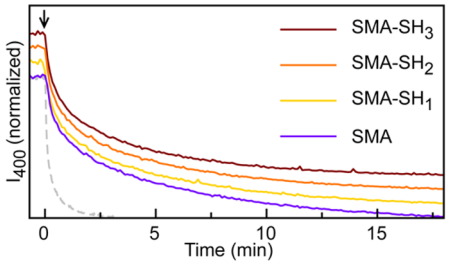

Figure 2. Liposome dissolution by SMA-SH$_x$ and SMA proceeds identically. The intensity of 400 nm light scattered by a solution of 0.05 mg/mL DMPC liposomes at 20 °C diminishes upon addition of up to 0.15 mg/mL SMA or SMA-SH$_x$ at t = 0 (indicated with an arrow). Each curve is normalized to the initial intensity and offset to facilitate comparison. The dashed gray line shows diminishing of light scattering upon addition of SMA at 25 °C.

the light scattered by this solution diminishes upon addition of a 3:1 (w/w) excess of SMA-SH$_x$ over DMPC, with a similar rate that is observed upon addition of the same amount of SMA. At 25 °C, this process occurs at a considerably increased rate (Figure 2; gray line).

We now turn to characterizing the product of SMA-SH-induced liposome dissolution. Briefly, 100 μL of a sample containing 5 mg/mL DMPC and 15 mg/mL SMA or SMA-SH$_x$ was injected into a Superdex 200 Increase 10/30 column to separate nanodiscs and excess polymer. Lipid nanodiscs elute predominantly between 11.3 and 13.8 mL after injection (Figure 3A), which corresponds to hydrodynamic radii between

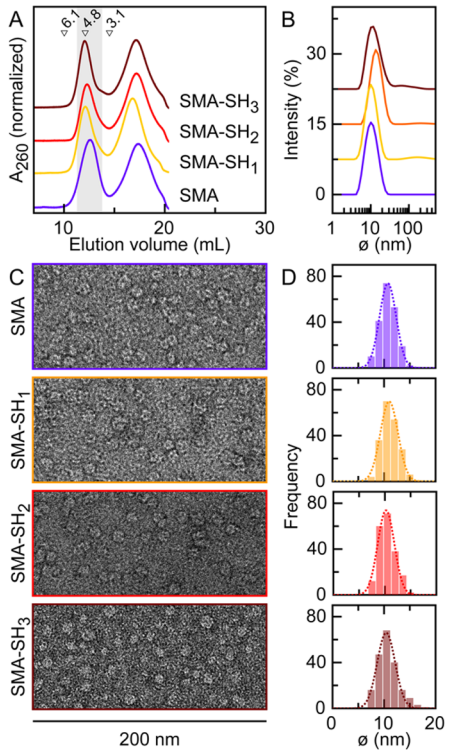

Figure 3. Like SMA, SMA-SH dissolves lipid bilayer membranes into lipid nanodiscs. (A) Elution profiles of SMA- and SMA-SH$_x$-DMPC nanodiscs obtained by analytical size-exclusion chromatography on a Superdex 200 Increase column. Numbers above the chromatograms indicate hydrodynamic radii (R_H; nm) corresponding to calibration standards. R_H of the majority of lipid nanodiscs ranges from 3.6 and 5.3 nm (indicated by the gray area). (B) Intensity-based particle diameter distributions, obtained from DLS analysis of SMA- and SMA-SH$_x$-DMPC nanodiscs eluting between 12.3 and 12.8 mL. Average particle diameters and corresponding standard deviations are 11.1 ± 4.0, 10.9 ± 3.6, 14.8 ± 5.0, and 13.5 ± 6.2 nm for SMA, SMA-SH$_1$, SMA-SH$_2$, and SMA-SH$_3$, respectively. (C) Representative negative stain transmission electron micrograph of SMA- and SMA-SH$_x$-DMPC nanodiscs. (D) TEM-based particle diameter distributions, obtained from measurement of 200 particles. Average particle diameters and corresponding standard deviations are 10.0 ± 1.6, 10.5 ± 2.0, 9.7 ± 1.6, and 10.1 ± 2.0 nm for SMA-, SMA-SH$_1$-, SMA-SH$_2$-, and SMA-SH$_3$-DMPC nanodiscs, respectively. Dotted lines represent the fit of a Gaussian distribution to the data.

~3.6 and ~5.3 nm. The excess of polymer that was included to ensure formation of nanodiscs of homogeneous size elutes at around 17.5 mL. Dynamic light scattering (DLS) reveals nearly identical particle diameter distributions for SMA-lipid nanodiscs and SMA-SH$_x$-lipid nanodiscs (Figure 3B). Transmission electron microscopy (TEM) micrographs reveal that SMA-SH$_x$-lipid nanodiscs appear as disc shaped particles, like their SMA-based counterparts, (Figure 3C and Supporting Information, S1) with a diameter of about 10 nm (Figure 3D).

SMA-SH Dissolves Proteoliposomes into Protein-Loaded Nanodiscs. Demonstration that SMA-SH can form protein-loaded nanodiscs emphasizes the potential of SMA-SH for characterization of membrane proteins. Applying our methodology to a membrane protein that is readily detected by, for instance, UV−vis spectroscopy benefits such demon-

DOI: 10.1021/acs.biomac.6b00140
Biomacromolecules 2016, 17, 1516−1522

stration. Therefore, we consider the protein bacteriorhodopsin (bR) from *Halobacterium salinarium*. This protein is the main protein component in the purple membrane (PM) of this photosynthesizing bacterium, and it has a retinal cofactor that absorbs light between 550 and 570 nm, which facilitates its detection. In addition, SMA was shown to form bR-loaded nanodiscs from bR-DMPC liposomes.[19,20]

bR-proteoliposomes are formed by adsorption of detergent from a ternary mixture of PM, *n*-octyl glucoside, and DMPC. This initially transparent solution becomes turbid during the reconstitution of bR into proteoliposomes. SMA- and SMA-SH_3-induced dissolution of the proteoliposomes results in clear purple solutions. These solutions remain purple after ultracentrifugation at 100000 × G for 1 h, whereas untreated proteoliposomes precipitate and no purple color is visible in the supernatant. This difference indicates that SMA and SMA-SH form bR-loaded nanodiscs, which is confirmed by subsequent analysis of the samples using gel filtration (Figure 4). In conclusion, grafting of SMA with cysteamine does not notably affect the membrane- and membrane-protein dissolving properties of SMA.

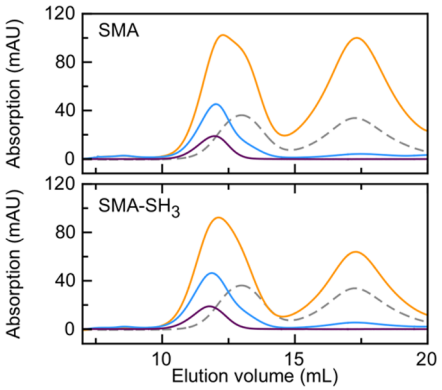

Figure 4. Size-exclusion chromatography reveals that SMA and SMA-SH dissolve bR from proteoliposomes into bR-loaded nanodiscs. A total of 500 μL of sample was injected onto a Superdex 200 Increase column, and absorption at 260 (orange), 280 (blue), and 565 nm (purple) was monitored. Compared to SMA-DMPC nanodiscs (gray dashes show absorption at 260 nm), SMA-bR and SMA-SH-bR nanodiscs elute at a lower volume and are characterized by an enhanced absorption at 280 and 565 nm.

Functionalization of SMA-SH-Lipid Nanodiscs. We modify SMA with cysteamine to produce a compound that tackles challenges in conjugation of membrane proteins with probes that are commonly used in biophysics assays, such as fluorophores and biotin. To assess whether SMA-SH-lipid nanodiscs sustain labeling with thiol-reactive probes, we use SMA-SH_3, because this SMA variant has the highest sulfhydril coverage (~0.6 sulfhydrils per molecule of SMA; see Figure 1). Below, we explore covalent modification of SMA-SH_3-DMPC nanodiscs with Alexa Fluor 488 C_5 maleimide (A488) and two thiol-reactive biotin derivatives.

A488 is a brightly fluorescent dye-label that can be used in (single-molecule) fluorescence experiments.[14,30−32] In the presence of a suitable acceptor, A488 can be used as donor fluorophore for Förster Resonance Energy Transfer (FRET). FRET is the nonradiative transfer of excitation energy from a donor fluorophore to an acceptor chromophore.[33−35] Presence of acceptor in proximity of donor results in a decreased donor fluorescence intensity compared to the donor fluorescence intensity in the absence of acceptor, because FRET acts as an additional nonradiative decay path for the excited donor. We use A488 as donor fluorophore and Atto647N as an acceptor. The Förster radius (R_0: the distance at which a FRET efficiency of 50% is expected) of this dye pair is about 4.9 nm (see Supporting Information, S2, for details on the R_0 calculation), which is compatible with the diameter of SMA-SH_3-lipid nanodiscs. Probing of energy transfer from donor that is covalently attached to the polymer bracelet to acceptor-labeled lipids within the SMA-SH_3-lipid nanodiscs requires comparison of the donor fluorescence intensity in absence and presence of acceptor, as shown schematically in Figure 5A. The donor-only sample is obtained by labeling of SMA-SH_3-DMPC nanodiscs with A488. The donor−acceptor sample is obtained by labeling of SMA-SH_3-DMPC nanodiscs that contain 1% Atto647N-labeled 1,2-dimyristoil-*sn*-glycero-3-phosphoethanolamine (Atto647N-DMPE) with A488.

Fluorescence emission and excitation spectra are obtained from solutions of these particles with identical donor label concentrations. Clearly, proximity of the acceptor label leads to a considerable reduction of the fluorescence emission intensity of the donor (Figure 5B). Using SMA-[DMPC + 1% Atto647N-DMPE] nanodiscs as acceptor-only control reveals that fluorescence emission of acceptor is negligible upon excitation between 450 and 550 nm (Figure 5C; dashed purple line). Thus, fluorescence photons with a wavelength of 680 nm

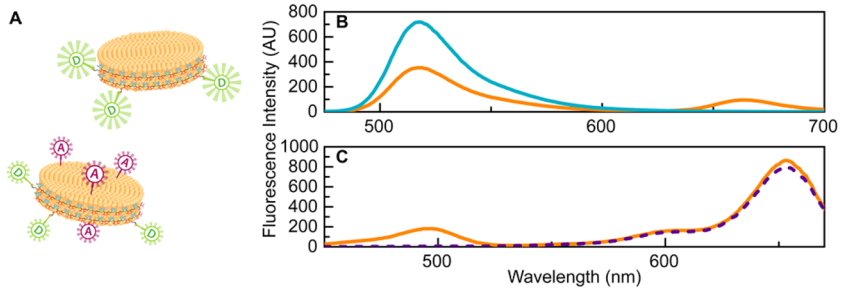

Figure 5. SMA-SH-lipid nanodiscs sustain covalent modification of sulfhydrils on the polymer that surrounds them. (A) Schematic representation of A488-labeled SMA-SH-DMPC nanodiscs in absence and presence of Atto647N-labeled DMPE (top and bottom, respectively). The donor and acceptor dyes are labeled with D and A, respectively. (B) Emission spectrum of A488-labeled SMA-SH-DMPC nanodiscs (cyan line) and A488-labeled SMA-SH_3-[DMPC + 1% Atto647N-DMPE] nanodiscs (orange line), upon excitation at 465 nm. (C) Excitation spectrum of A488-labeled SMA-SH_3-[DMPC + 1% Atto647N-DMPE] nanodiscs (orange line) and SMA-[DMPC + 1% Atto647N-DMPE] nanodiscs (dashed purple line), monitored at 680 nm.

DOI: 10.1021/acs.biomac.6b00140
Biomacromolecules 2016, 17, 1516−1522

that arise upon excitation between 450 and 550 nm (Figure 5B,C; orange line) arise from excitation of the acceptor through FRET. FRET demonstrates that A488, which is on the polymer surrounding the lipid nanodiscs, and Atto647N-labeled lipids are within the same particle. Thus, SMA-SH_3-lipid nanodiscs sustain covalent modification with A488.

Tethering of proteins to a surface enables studying their dynamics using, for example, fluorescence microscopy[13] and optical tweezers.[36] This immobilization is commonly mediated by the interaction between the protein avidin and its ligand biotin and generally involves covalent attachment of a biotin-derivative to the protein of interest. Commercially available thiol-reactive biotin derivatives mostly differ in the composition and length of the spacer-arm that separates the biotin from the thiol-reactive moiety. Here, we assess use of biotin-maleimide and maleimide-PEG_{11}-biotin, in which maleimide and biotin are separated by ∼2 and ∼6 nm, respectively.

DyLight488-labeled avidin (D488-avidin) is used as a reporter for binding of biotinylated SMA-SH_3-lipid nanodiscs. DyLight488 is spectrally similar to A488 and can, therefore, serve as a FRET-donor to Atto647N-labeled lipids within the nanodiscs, as shown schematically in Figure 6A. SMA-SH_3-[DMPC + 1% Atto647N-DMPE] nanodiscs were labeled with either biotin-maleimide or maleimide-PEG_{11}-biotin, to obtain two different variants of biotinylated lipid nanodiscs. D488-avidin that was incubated with excess biotin prior to addition of biotinylated lipid nanodiscs serves as a donor-only sample (Figure 6B; purple line). Biotinylated lipid-nanodiscs were added to this sample to verify that only specific interaction between D488-avidin and biotinylated lipid nanodiscs contribute to changes in donor fluorescence intensity.

The fluorescence intensity of D488-avidin decreases by ∼20% upon addition of maleimide-PEG_{11}-biotin-labeled SMA-SH_3-[DMPC + 1% Atto647N-DMPE] nanodiscs (Figure 6B; cyan line), because the excited donor on D488-avidin transfers energy to Atto647N-labeled lipids. The efficiency of energy transfer is inversely proportional to the distance between donor and acceptor. Indeed, addition of biotin-maleimide labeled SMA-SH_3-[DMPC + 1% Atto647N-DMPE] nanodiscs, in which the spacer arm that separates biotin from maleimide is considerably shorter than in maleimide-PEG_{11}-biotin, results in a decrease of donor fluorescence intensity of nearly 40% (Figure 6B; orange line). Thus, SMA-SH_3-lipid nanodiscs sustain covalent modification with two different biotinylation agents.

The results above indicate that SMA-SH-lipid nanodiscs can be functionalized with thiol-reactive probes.

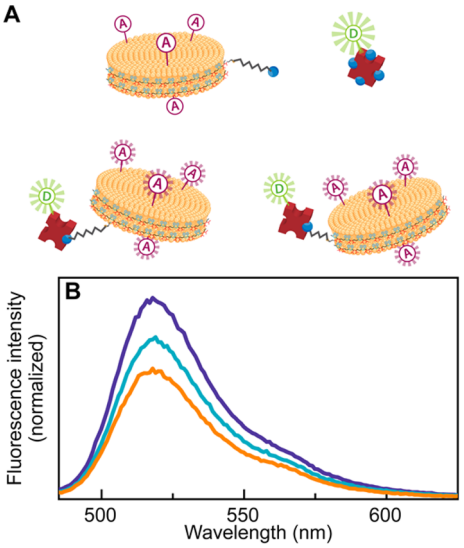

Figure 6. Fluorescence of DyLight488-labeled avidin decreases upon interaction with biotinylated SMA-SH3-DMPC nanodiscs that contain 1% Atto647N-DMPE. (A) Schematic representation of interaction between D488-avidin and biotinylated nanodiscs. Binding of biotin to D488-avidin prevents interaction with biotinylated nanodiscs (top). Interaction between D488-avidin and SMA-SH_3-[DMPC + 1% Atto647N-DMPE] nanodiscs that are biotinylated with either maleimide-PEG_{11}-biotin or biotin-maleimide to D488-avidin (bottom left and right, respectively) results in formation of complexes in which avidin and the nanodisc are separated by a different distance. (B) Fluorescence emission spectrum of D488-avidin that was incubated with excess biotin prior to addition of biotinylated SMA-SH_3-[DMPC + 1% Atto647N-DMPE] nanodiscs (purple) and D488-avidin after addition of SMA-SH_3-[DMPC + 1% Atto647N-DMPE] nanodiscs that are biotinylated with maleimide-PEG_{11}-biotin (cyan) and biotin-maleimide (orange). Fluorescence intensities are normalized to the spectra obtained for D488-avidin that was incubated with excess biotin prior to addition of biotinylated SMA-SH_3-[DMPC + 1% Atto647N-DMPE] nanodiscs.

CONCLUSION

Challenges in purification and functionalization of membrane proteins complicate their biochemical and biophysical characterization. The recently discovered application of the amphipathic styrene-maleic acid copolymer for detergent-free purification of membrane proteins has the potential to greatly facilitate membrane protein purification. We sought to facilitate functionalization of those membrane proteins, and modified the polymer with cysteamine for this purpose. The product of this modification is SMA-SH: a variant of SMA that is grafted with sulfhydrils. The amount of cysteamine included in the reaction tunes the thiol-content of SMA-SH. SMA-SH dissolves liposomes into nanosized discs just like SMA does. In addition, SMA-SH is, just like SMA, capable of dissolving proteoliposomes into protein-loaded nanodiscs. However, unlike SMA-lipid nanodiscs, SMA-SH-lipid nanodiscs are susceptible to, and sustain, covalent attachment of thiol-reactive derivatives of functional compounds, such as biotin and fluorophores. Although control over label numbers and position is more limited in case of the SMA-SH approach than in case of site-specific modification of an engineered protein, SMA-SH does not require preparation of engineered membrane protein variants. Thus, the results presented here highlight the potential of SMA-SH to simplify biophysical characterization of membrane proteins.

Despite the presence of solvent-accessible sulfhydrils on the polymer, thiol-reactive compounds may also react with cysteine residues within the protein that is embedded in the lipid nanodisc. To prevent such undesired cross-reactivity, one could employ the same chemistry as used here to modify SMA with compounds that enable more selective reactions, like amine derivatives of functional groups used for click chemistry (alkyne, alkene, etc.). However, this enhanced selectivity comes at a price, because these compounds are generally orders of magnitude more expensive than cysteamine. In contrast, production of SMA-SH is cheap and can be carried out in any reasonably equipped (bio)chemistry laboratory. Therefore, we anticipate that our SMA-SH approach will find

DOI: 10.1021/acs.biomac.6b00140
Biomacromolecules 2016, 17, 1516−1522

application in many biochemical and biophysical approaches that involve conjugation of membrane proteins.

■ ASSOCIATED CONTENT

Supporting Information

The Supporting Information is available free of charge on the ACS Publications website at DOI: 10.1021/acs.biomac.6b00140.

S1 includes transmission electron micrographs of SMA-lipid nanodiscs and SMA-SH_x-lipid nanodiscs. S2 includes the calculation of the Forster radius of Alexa488-Atto647N (PDF).

■ AUTHOR INFORMATION

Corresponding Authors

*E-mail: s.lindhoud@tudelft.nl.
*E-mail: m.e.aubin-tam@tudelft.nl.

Notes

The authors declare no competing financial interest.

■ ACKNOWLEDGMENTS

M.E.A. received financial support from a Marie Curie CiG Grant (618454) and a Netherlands Organization for Scientific Research VENI Grant (722.013.006). We gratefully acknowledge Andreas Engel for his advice and critical reading of the manuscript.

■ ABBREVIATIONS

SMA, styrene-maleic acid copolymer; SMA-SH, SMA that is modified with cysteamine; SMAnh, styrene-maleic anhydride copolymer; DTT, dithiothreitol; DMPC, 1,2-dimyristoil-*sn*-glycero-3 phosphocholine; Atto647N DMPE, Atto647N-labeled 1,2-dimyristoil-*sn*-glycero-3 phosphoethanolamine; DLS, dynamic light scattering; TEM, transmission electron micropscopy; FRET, Förster resonance energy transfer; A488, Alexa Fluor 488 C_5 maleimide; D488-avidin, DyLight488-labeled avidin; Et_3N, triethylamine; DTNB, dithionitrobenzoicacid; PM, purple membrane; bR, bacteriorhodopsin

■ REFERENCES

(1) Seddon, A. M.; Curnow, P.; Booth, P. J. *Biochim. Biophys. Acta, Biomembr.* **2004**, *1666*, 105.
(2) Lee, A. G. *Biochim. Biophys. Acta, Biomembr.* **2004**, *1666*, 62.
(3) Yeagle, P. L. *Biochim. Biophys. Acta, Biomembr.* **2014**, *1838*, 1548.
(4) Whitelegge, J. P. *Anal. Chem.* **2013**, *85*, 2558.
(5) Laganowsky, A.; Reading, E.; Allison, T. M.; Ulmschneider, M. B.; Degiacomi, M. T.; Baldwin, A. J.; Robinson, C. V. *Nature* **2014**, *510*, 172.
(6) Erkens, G. B.; Hanelt, I.; Goudsmits, J. M.; Slotboom, D. J.; van Oijen, A. M. *Nature* **2013**, *502*, 119.
(7) Bayburt, T. H.; Sligar, S. G. *FEBS Lett.* **2010**, *584*, 1721.
(8) Ritchie, T. K.; Grinkova, Y. V.; Bayburt, T. H.; Denisov, I. G.; Zolnerciks, J. K.; Atkins, W. M.; Sligar, S. G. *Methods Enzymol.* **2009**, *464*, 211.
(9) Nath, A.; Trexler, A. J.; Koo, P.; Miranker, A. D.; Atkins, W. M.; Rhoades, E. *Methods Enzymol.* **2010**, *472*, 89.
(10) Dorr, J. M.; Scheidelaar, S.; Koorengevel, M. C.; Dominguez, J. J.; Schafer, M.; van Walree, C. A.; Killian, J. A. *Eur. Biophys. J.* **2016**, *45*, 3.
(11) Gluck, J. M.; Koenig, B. W.; Willbold, D. *Anal. Biochem.* **2011**, *408*, 46.
(12) Zocher, M.; Roos, C.; Wegmann, S.; Bosshart, P. D.; Dotsch, V.; Bernhard, F.; Muller, D. J. *ACS Nano* **2012**, *6*, 961.
(13) Gouridis, G.; Schuurman-Wolters, G. K.; Ploetz, E.; Husada, F.; Vietrov, R.; de Boer, M.; Cordes, T.; Poolman, B. *Nat. Struct. Mol. Biol.* **2014**, *22*, 57.
(14) Schuler, B.; Lipman, E. A.; Steinbach, P. J.; Kumke, M.; Eaton, W. A. *Proc. Natl. Acad. Sci. U. S. A.* **2005**, *102*, 2754.
(15) Rhoades, E.; Gussakovsky, E.; Haran, G. *Proc. Natl. Acad. Sci. U. S. A.* **2003**, *100*, 3197.
(16) Pirchi, M.; Ziv, G.; Riven, I.; Cohen, S. S.; Zohar, N.; Barak, Y.; Haran, G. *Nat. Commun.* **2011**, *2*, 493.
(17) Gulati, S.; Jamshad, M.; Knowles, T. J.; Morrison, K. A.; Downing, R.; Cant, N.; Collins, R.; Koenderink, J. B.; Ford, R. C.; Overduin, M.; Kerr, I. D.; Dafforn, T. R.; Rothnie, A. J. *Biochem. J.* **2014**, *461*, 269.
(18) Jamshad, M.; Lin, Y. P.; Knowles, T. J.; Parslow, R. A.; Harris, C.; Wheatley, M.; Poyner, D. R.; Bill, R. M.; Thomas, O. R.; Overduin, M.; Dafforn, T. R. *Biochem. Soc. Trans.* **2011**, *39*, 813.
(19) Knowles, T. J.; Finka, R.; Smith, C.; Lin, Y. P.; Dafforn, T.; Overduin, M. *J. Am. Chem. Soc.* **2009**, *131*, 7484.
(20) Orwick-Rydmark, M.; Lovett, J. E.; Graziadei, A.; Lindholm, L.; Hicks, M. R.; Watts, A. *Nano Lett.* **2012**, *12*, 4687.
(21) Orwick, M. C.; Judge, P. J.; Procek, J.; Lindholm, L.; Graziadei, A.; Engel, A.; Grobner, G.; Watts, A. *Angew. Chem., Int. Ed.* **2012**, *51*, 4653.
(22) Swainsbury, D. J.; Scheidelaar, S.; van Grondelle, R.; Killian, J. A.; Jones, M. R. *Angew. Chem., Int. Ed.* **2014**, *53*, 11803.
(23) Dorr, J. M.; Koorengevel, M. C.; Schafer, M.; Prokofyev, A. V.; Scheidelaar, S.; van der Cruijsen, E. A.; Dafforn, T. R.; Baldus, M.; Killian, J. A. *Proc. Natl. Acad. Sci. U. S. A.* **2014**, *111*, 18607.
(24) Prabudiansyah, I.; Kusters, I.; Caforio, A.; Driessen, A. J. *Biochim. Biophys. Acta, Biomembr.* **2015**, *1848*, 2050.
(25) Henry, S. M.; El-Sayed, M. E.; Pirie, C. M.; Hoffman, A. S.; Stayton, P. S. *Biomacromolecules* **2006**, *7*, 2407.
(26) Mu, Y.; Kamada, H.; Kaneda, Y.; Yamamoto, Y.; Kodaira, H.; Tsunoda, S.; Tsutsumi, Y.; Maeda, M.; Kawasaki, K.; Nomizu, M.; Yamada, Y.; Mayumi, T. *Biochem. Biophys. Res. Commun.* **1999**, *255*, 75.
(27) Li, Z.; Song, Y. L.; Yang, Y. H.; Yang, L.; Huang, X. H.; Han, J. H.; Han, S. F. *Chem. Sci.* **2012**, *3*, 2941.
(28) de Vos, W. M.; Leermakers, F. A. M. *Polymer* **2009**, *50*, 305.
(29) Zhang, R.; Sahu, I. D.; Liu, L.; Osatuke, A.; Comer, R. G.; Dabney-Smith, C.; Lorigan, G. A. *Biochim. Biophys. Acta, Biomembr.* **2015**, *1848*, 329.
(30) Lindhoud, S.; Pirchi, M.; Westphal, A. H.; Haran, G.; van Mierlo, C. P. M. *J. Mol. Biol.* **2015**, *427*, 3148.
(31) Lindhoud, S.; Westphal, A. H.; Visser, A. J. W. G.; Borst, J. W.; van Mierlo, C. P. M. *PLoS One* **2012**, *7*, e46838.
(32) Panchuk-Voloshina, N.; Haugland, R. P.; Bishop-Stewart, J.; Bhalgat, M. K.; Millard, P. J.; Mao, F.; Leung, W. Y.; Haugland, R. P. *J. Histochem. Cytochem.* **1999**, *47*, 1179.
(33) Forster, T. *Ann. Phys.* **1948**, *2*, 55.
(34) Stryer, L. *Annu. Rev. Biochem.* **1978**, *47*, 819.
(35) Stryer, L.; Haugland, R. P. *Proc. Natl. Acad. Sci. U. S. A.* **1967**, *58*, 719.
(36) Aubin-Tam, M. E.; Olivares, A. O.; Sauer, R. T.; Baker, T. A.; Lang, M. J. *Cell* **2011**, *145*, 257.

DOI: 10.1021/acs.biomac.6b00140
Biomacromolecules 2016, 17, 1516−1522